Eur. Phys. J. D **3**, 29–41 (1998)

THE EUROPEAN PHYSICAL JOURNAL D

Relativistic and many-body effects in K, L, and M shell ionization energy for elements with $10 \leq Z \leq 100$ and the determination of the 1s Lamb shift for heavy elements

P. Indelicato[1,a], S. Boucard[1], and E. Lindroth[2]

[1] Laboratoire Kastler-Brossel[b], École Normale Supérieure et Université Pierre et Marie Curie, Case 74, 4 place Jussieu, 75252 Paris Cedex 05, France
[2] Department of Atomic Physics, Stockholm University, 104 05 Stockholm, Sweden

Received: 25 February 1998 / Accepted: 31 March 1998

Abstract. We report on a calculation of K, L and M inner-shell ionization energy in atoms with atomic numbers in the range $10 \leq Z \leq 100$. Many-body effects are evaluated for all $n = 1$, 2, and 3 hole states. Those include correlation and effects due to the auto-ionizing nature of the hole states (Auger shift). For high Z we add recent corrected nuclear polarization, and several second-order vacuum polarization corrections. K and L ionization energies are compared with experimental X-ray absorption edges measurements. Excellent agreement with rare gazes and metal vapor measurements is found. We also compare our calculations with X-ray transition energies for all K and L lines that involve K, L and M holes. Finally we use K X-ray lines to deduce an hydrogenlike $1s$ Lamb shift for several heavy elements, with far better accuracy than has been obtained by direct measurements of hydrogenlike ions.

PACS. 31.10.+z Theory of electronic structure, electronic transitions, and chemical binding – 31.15.Ar Ab initio calculations – 31.30.Jv Relativistic and quantum elecrodynamic effects in atoms and molecules

Introduction

In a previous paper [1], we have reported on an *ab initio* calculation of Kα transition energy for some atoms with atomic number in the range $30 \leq Z \leq 100$. We also performed a complete calculation of K and L transitions involving K, L and M electrons in Xe [2] and we explored Kβ transition in more recent work [3,4]. These calculations includes relativistic effects, QED corrections, many-body corrections including those due to the auto-ionizing nature of the hole states (Auger shift). The study of inner-shell transitions in heavy atom has became one of the most promising tool to test QED in strong Coulomb field, now that it has been shown [1,2] that the full complexity of the relativistic many-body problem with up to ≈ 100 electrons can be addressed. While the precision of the best measurement of the $2p \rightarrow 1s$ transition energy in hydrogenlike uranium is 16 eV [5,6], we can compare our calculations with experiments the precision of which is in the 0.2–2 eV range [7] for thorium, uranium and several transuranic elements. The consequences of such accurate calculations for our understanding of QED in strong Coulomb fields have been discussed in detail in [8].

Moreover such large scale, high-precision calculations can be used to improve X-ray transition energies tables that are in widespread use (from crystallography to analytical chemistry) by comparing the calculation to selected sets of reliable experimental data. One can then construct an experimental correction curve that will account for uncalculated effects and use it to identify low precision or faulty experiments or low precision interpolations for lines which have never been directly measured. It appears that current tables [9] have many very inaccurate, or mis-identified lines, most of which have been measured only once in the early part of the century. While it would be a huge effort to systematically remeasure all the lines appearing in those tables, which have not yet been firmly established, a correction curve built on the present calculation can point to the places where such remeasurements are in order, or provide better semi-empirical energies. An other challenging topic that we address in the present work, is the calculation of ionization energies. Cancelation that occurs in transitions, does not necessarily happen for ionization energies. Also ionization energies are more sensitive to the environment than transition energies. Comparing gas or solid phase measurements can thus provide very interesting insights on solid-state effects.

In the present work we use the method of calculation described in references [1,2] to evaluate all K, L, and M ionization energies and extend our previous work toward

[a] e-mail: paul@spectro.jussieu.fr
[b] Unité Associée No. 18 du CNRS

lower Z. Indeed it also allows us to calculate several L transition energies that were not at all calculated except for Xe [2]. The Auger shift of the $3s^{-1}$ and $3p^{-1}$ levels are expected to be larger than those of the $2p^{-1}$ and thus Kβ and L transitions should provide an excellent test of this part of the calculation. The calculation of the Auger shift is done with a new method that has been developed for the study of doubly excited resonances in few-electron systems [10,11] and proven to be very accurate in comparison with experiments. In lighter elements correlation effects are expected to be more important, and thus again it should provide a good test of our calculation.

This paper is arranged as follows. In Section 1 we describe briefly what has been taken into account in the calculation. In Section 2 we tabulate results and make a detailed comparison with experiment. In Section 3 we describe how to obtain the "hydrogenic" $1s$ Lamb shift from the present work and compare it to results obtained from direct measurements on ions.

1 Principle of the calculation

In the present section we describe the various contributions that are used in the calculation. Our aim is to provide an accurate description of the autoionizing states with holes in $n = 1$, 2 and 3, involved in the K and L transitions, *i.e.* Kα_1, Kα_2, Kβ_1, Kβ_3, Lα_1, Lα_2, Lβ_1, Lβ_3, Lβ_4, Lβ_9, Lβ_{10}, Lβ_{17}, Lη, Ll, Ls and Lt. All 9 subshells are involved ($1s_{1/2}$, $2s_{1/2}$, $2p_{1/2}$, $2p_{3/2}$, $3s_{1/2}$, $3p_{1/2}$, $3p_{3/2}$, $3d_{3/2}$, and $3d_{5/2}$) either as initial or final states, for this group of transitions, thus leading to a complete description of the 3 lower shells of the atom. The correspondence between line designation in Siegbahn notation and spectroscopic notation is shown in Table 1. Since we start at $Z = 10$, the 9 levels will not all be present for the smaller Z, and the full complement will be reached only around $Z = 25$.

1.1 Zeroth-order energy and QED corrections

Our starting point is the fully relaxed Dirac-Fock energy. Coupling of the open inner-shells to the outer shell is neglected in order to make the calculation manageable. We also use pure jj coupling to avoid getting unmanageably large calculations. This approximation shows itself only at the lower Z range. In a limited number of cases (iodine or copper for example) one may have to rearrange the electrons in the open outer shells to avoid getting two open shells with identical angular quantum numbers and identical numbers of electrons (for example in iodine $2p_{3/2}^{-1}$ and $5p_{3/2}^{-1}$), otherwise convergence of the SCF (self-consistent field) process cannot be obtained. In this case obviously the same arrangement is used for all 9 levels. This method gives very good results for transition energies, but not for ionization energies. In all the cases with that kind of problem, we calculate all levels with the correct outer-shell structure for which the symmetry does not lead to convergence problems and use the average difference between both calculation to correct the levels for which convergence cannot be achieved. Example of changes in ionization energy for a few selected elements due to that procedure are shown in Table 2. From this table it can be seen that rearranging the outermost electrons in Cu, for which the $4d$ shell is closed, gives an almost constant shift which thus affects only ionization energies but not transition energies. It is thus easy to correct all ionization energies by adding the average shift to level energies that cannot be calculated directly. In contrast, when the $3d$ shell is being rearranged as in Cr, the shift is larger and shell dependent. In that case the calculated value for both the transition and ionization energies is unreliable, and corrections for levels that cannot be calculated directly can only be guessed. Here we use the shift from the closest shell to make the correction.

Table 1. Correspondence between Siegbahn and IUPAP line names and levels names for the lines that can be calculated from the present work.

Siegbahn	IUPAC	Initial State	Final State
Kα_1	KL_3	$1s^{-1}$	$2p_{3/2}^{-1}$
K$\alpha 2$	KL_2	$1s^{-1}$	$2p_{1/2}^{-1}$
Kβ_1	KM_3	$1s^{-1}$	$3p_{3/2}^{-1}$
K$\beta 3$	KM_2	$1s^{-1}$	$3p_{1/2}^{-1}$
Lα_1	L_3M_5	$2p_{3/2}^{-1}$	$3d_{5/2}^{-1}$
Lα_2	L_3M_4	$2p_{3/2}^{-1}$	$3d_{3/2}^{-1}$
Lβ_1	L_2M_4	$2p_{1/2}^{-1}$	$3d_{3/2}^{-1}$
Lβ_3	L_1M_3	$2s^{-1}$	$3p_{3/2}^{-1}$
Lβ_4	L_1M_2	$2s^{-1}$	$3p_{1/2}^{-1}$
Lβ_9	L_1M_5	$2s^{-1}$	$3d_{5/2}^{-1}$
Lβ_{10}	L_1M_4	$2s^{-1}$	$3d_{3/2}^{-1}$
Lβ_{17}	L_2M_3	$2p_{1/2}^{-1}$	$3p_{3/2}^{-1}$
Lη	L_2M_1	$2p_{1/2}^{-1}$	$3s^{-1}$
Ll	L_3M_1	$2p_{3/2}^{-1}$	$3s^{-1}$
Lt	L_3M_2	$2p_{3/2}^{-1}$	$3p_{1/2}^{-1}$

In order to get better accuracy at high-Z the wave functions are calculated with both the Coulomb and the magnetic (Gaunt) interactions in the self-consistent field. Retardation to all orders in v/c is included as a first order perturbation.

Finite nuclear size is also included, using experimental nuclear radii when available, or Johnson and Soff interpolation formula. For heavy elements beyond thorium, the effect of nuclear deformation on the mean square charge radius are included [12–14] in the same spirit as in reference [15]. It has been shown [1,16] that it leads to a much better agreement between theory and experiment at high Z for Kα transitions. In heavy element it has been thought that the energy shift due to the polarization of the nucleus by the atomic electron could be important ($\approx$ 1 eV). It has been calculated first for U [17], then U and Pb [18], and recently for several transuranic elements.

Table 2. Effect of changes in the outer shell structure on the ionization energy of K, L and M shell (eV). Missing numbers correspond to calculation which could not converge in the correct outer shell configuration. * in orbital labels corresponds to the orbital with $j = l - 1/2$.

	Outer-Shell change	$1s$	$2s$	$2p_{1/2}$	$2p_{3/2}$	$3s$	$3p_{1/2}$	$3p_{3/2}$	$3d_{3/2}$	$3d_{5/2}$
Na	$3d* \to 3s$			4.46	4.45					
Al	$3d* \to 3p*$	5.05	4.52		4.56	2.48				
Cl	$2p^2 3d \to 2p^3$	7.32	6.29	6.59		3.87	4.93	4.58		
K	$3d* \to 4s$			−1.28	−1.44		−0.10	−0.78		
Cr	$3d^6 \to 3d^5 4s$			7.24	6.68		6.08	4.70	5.03	
Cu	$3d^{10}4p \to 3d^{10}4s$			2.18	2.19		2.25	2.29	2.19	2.22
Br	$4p^2 4d \to 4p^3$	6.20	5.96	6.04		5.82	5.89		5.88	5.75
Rb	$5s \to 4d*$			−0.48	−0.52		−0.52	−0.54	−0.45	−0.53
Nb	$5s4d*^4 \to 4d*^4 4d$			−0.81	−0.68		−0.77	−0.72	−0.84	−0.60
Mo	$5s4d*^4 4d \to 4d*^4 4d^2$			4.24	4.10		4.15	4.09	4.22	3.94
I	$5p^2 5d \to 5p^3$	4.33	4.21	4.25		4.16	4.19		4.20	4.16
Cs	$5d* \to 6s$			−1.11	−1.13		−1.12	−1.13	−1.09	−1.13
La	$5d \to 5d*$	0.11	0.11	0.06	0.14	0.10	0.09	0.11	0.04	0.15
Ir	$5p^2 5d \to 5p^3$	6.37	6.71	6.71	6.62	6.71	6.67	6.64	6.71	
Pt	$5d^8 6s^2 \to 5d^9 6s$			3.75	3.70		3.72	3.70	3.75	
Au	$5d^{10}5f* \to 5d^{10}6s$			6.61	6.60		6.60	6.60	6.60	6.61
Tl	$6p* \to 5f*$	6.20	6.11		6.11	6.09		6.09	6.08	6.09
At	$6p*^2 6p^2 6d* \to 6p*26p3$	4.08	4.02	4.04		4.00	4.01		4.01	4.00
Fr	$6d* \to 7s$			−0.38	−0.39		−0.39	−0.39	−0.38	−0.39
Bk	$7s^2 5f*^6 5f^3 \to 7s^2 5f*^6 5f^2 6d*$	−5.04	−5.39	−5.32	−5.39	−5.82	−5.85	−5.78	−5.90	−5.68

It appears however that the value tabulated in all three previous reference must be divided by 2π, which makes the nuclear polarization a negligible correction [19]. We include it nevertheless for all elements for which it has been evaluated.

QED corrections are an important contribution for medium to high Z elements. These corrections can be divided in one and two-electron corrections. Self-energy and vacuum polarization (Fig. 1) are the two first order one-electron corrections, and behave as $\alpha(Z\alpha)^4$. Second-order one-electron radiative corrections (Fig. 2) behave as $\alpha^2(Z\alpha)^4$ and $\alpha^2(Z\alpha)^5$ and can be important at high-Z, while lowest order two-body corrections behave as $\alpha^2(Z\alpha)^3$ (Fig. 3). The QED part of the two-photon electron-electron interaction (Fig. 4) contributes in the same order. Only a small number of these contributions has been evaluated, and often they are known only for low Z, or for two-electron systems. There is no way that we can include them in a consistent fashion. We thus decided to include all correction that can be calculated, even though some corrections of the same order in α cannot be included. The reason to do so is that corrections formally of the same order in α can be of very different size.

Here we include the dominant self-energy [20–22] and vacuum polarization with finite nuclear size correction. Among the second order one-electron corrections we include (Fig. 2) the Källén and Sabry two-loop vacuum polarization and the iterated vacuum polarization (in the Uehling approximation), obtained by adding the Uehling potential in the self-consistent process. This calculation gives very precisely the same results as direct QED evaluation [23].

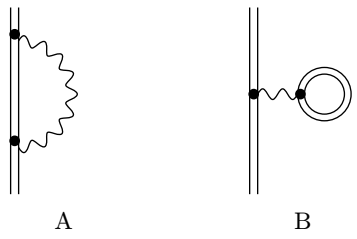

Fig. 1. Feynman diagrams for self-energy (A) and vacuum polarization (B) (contributions of order $\alpha(Z\alpha)^4$).

There are other radiative corrections that have not yet been calculated, or which are known only for $Z = 92$. Only the irreducible part of the two-loop self-energy has been evaluated, and the remaining reducible part may be the largest unknown contribution to one-electron radiative corrections. Mixed self-energy vacuum polarization diagrams have been calculated for $Z = 92$. In this work we scale the value from reference [24] by $(Z\alpha)^5$ to

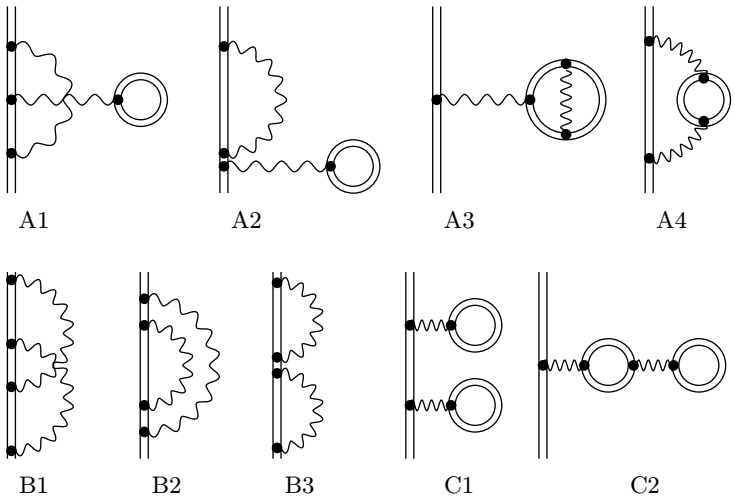

Fig. 2. Second-order one-electron Feynman diagrams for radiative corrections. Only the Källén and Sabry contribution (A3+C2) and iterated Uelhing contribution (C1) are included in the present work.

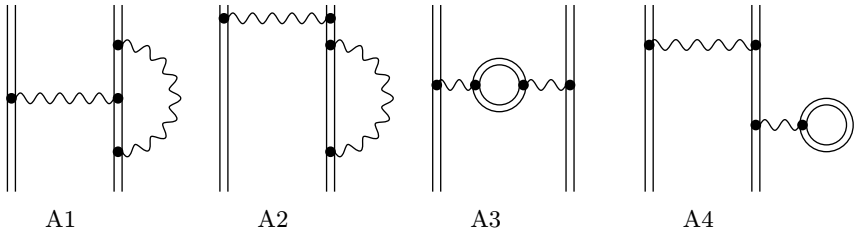

Fig. 3. Feynman diagrams for the radiative corrections to the electron-electron interaction (order $\alpha^2(Z\alpha)^3$).

account for this correction at other Z values. The QED part of the two-photon electron-electron interaction is also left out, since this correction has only be evaluated for the ground state of two-electron ions [24,25]. Finally the radiative correction to the electron-electron interaction are included in the Welton approximation, as described in our earlier work. The sum of these missing QED corrections dominate the theoretical uncertainty for $Z > 90$ and could add up to a few eV.

1.2 Many-body effects

Several many-body effects have to be accounted for. We use relativistic many-body perturbation theory to calculate *correlation*, which we call the admixture of configurations with two excited orbitals, as well as *core-core* and *Auger-effects*, which denote admixture of configurations with two holes different from the original hole. The correlation contribution to the binding energy of a deep core electron is rather small due to the large energy associated with the promotion of the electron to an unoccupied level, and it has a smooth Z-dependence all over the periodic table. Coulomb and Breit correlation, obtained with second order many-body perturbation theory, are presented in Figure 5.

Admixture of two holes, on the other hand, can sometimes be rather important and shows further a substantial variation over the periodic table. Important contributions arise especially when the energy of the single hole state considered is close to the energy of the admixed state with two holes, such that ejection of a low energy Auger electron is allowed, or nearly allowed. From a computational viewpoint it is natural to classify these admixture into two classes. One class includes the admixture that consist of pairs of core electrons, which together have a larger binding energy than the single hole (core-core effects). The other class, the Auger effects, is due to electron pairs that have small enough binding energy to undergo a real Auger transition. The latter class is more complicated to calculate since the autoionizing property of the vacancy state has to be accounted for. For this purpose we

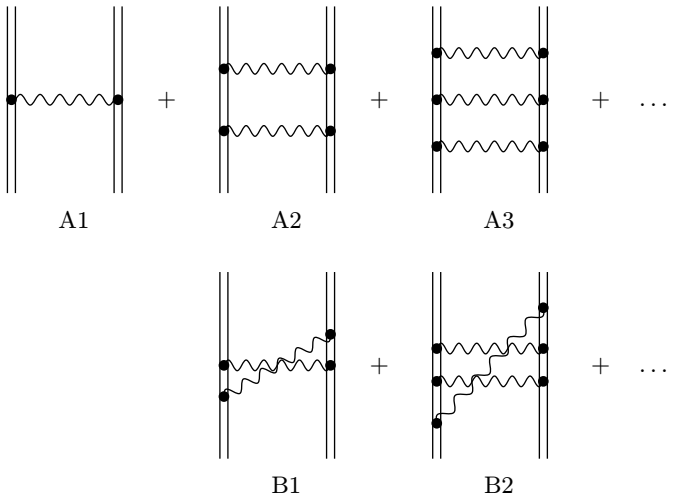

Fig. 4. Feynman diagrams for the ladder and crossed-ladder approximation. The complete one photon contribution, as well as the exact non-QED part of the two-photon ladder diagrams are included in the present work. Fraction of the contribution of higher order ladder diagrams are also included.

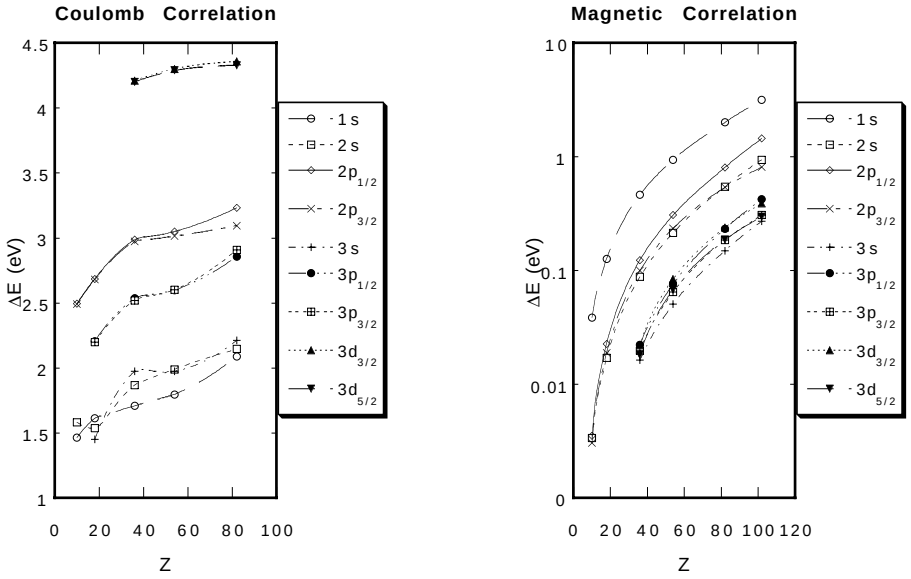

Fig. 5. Coulomb and Magnetic correlation contributions to K, L and M ionization energies (eV).

use the method of complex rotation, which is here combined with relativistic many-body perturbation theory in second order, see references [10,11] for details.

Coulomb and Gaunt correlation are presented in Figure 5. The sum of core-core and Auger shift are shown in Figure 6 for all shells studied here.

2 Results and discussion

The selection of experimental data for a detailed comparison between experiment and theory is not straightforward. In our previous work [1] on Kα transitions, we had made calculations only for elements for which we knew trustworthy data existed, except for very high-Z, where we used all available data. The trustworthy data included data connected to well established standard lines by the mean of reliable experimental methods, or absolute measurements. In some cases old measurement had to be reevaluated using newer standard for X or γ-rays energies or updated fundamental constants [1]. Here we have calculated many more elements, for which no such data is known. In this case we could only resort to a direct use of Bearden's tables [9], even though it is well known that it contains in

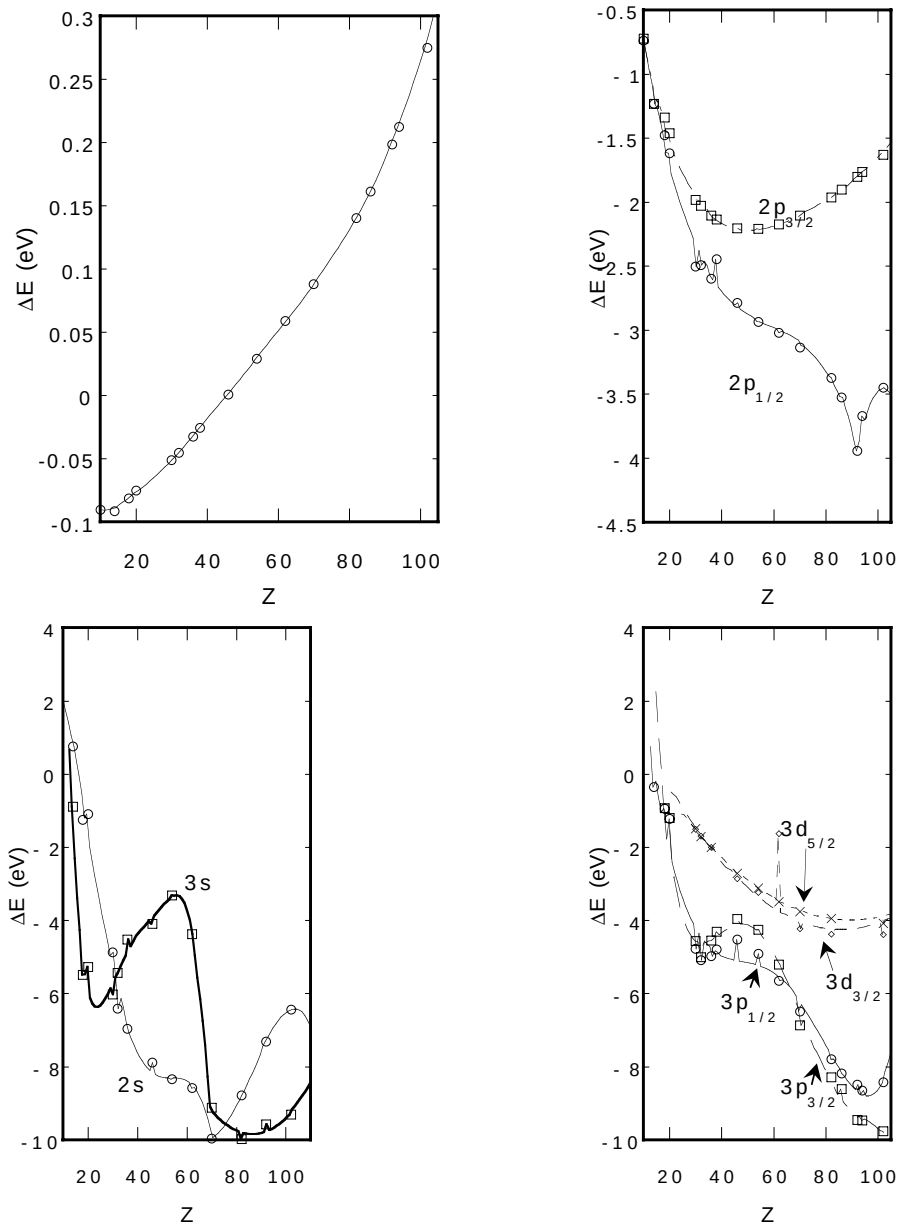

Fig. 6. Sum of the core-core and Auger shift contributions to to K, L and M ionization energies energies (eV).

some cases data of poor reliability. For many lines and elements in that category we have been able to use a recent partial reevaluation [26] of Bearden's tables which uses modern measurement and updated fundamental constants. This table also provides improved K and L absorption edges. When the line used was not reevaluated in reference [26], we used the same procedure to connect it to known standards. For light elements, recent measurements have appeared [27–30], which enabled us to do a valid comparison down to $Z = 10$. These new measurements together with a few unpublished results are included in reference [26].

Theoretical ionization energies for all calculated elements and levels are presented in Tables 3 and 4. The differences between theoretical and experimental values for K, L and M absorption edges are plotted in Figure 7. In this figure, we have emphasized the case of rare gas or metallic vapor measurements. Those are in general good agreement with theory (within 1 eV most of the time). Measurements done with solids are in worse agreement, because of changes in the external structure of the ion, compared to isolated ions. These are the well known chemical and solid state shifts.

Experiment-Theory curves for K and L transition energies that can be calculated from differences of K, L, and M ionization energies from Tables 3 and 4 are presented in Figures 8 to 10. The meaning of this notation in term of shell labels is explained in Table 1. The agreement

Table 3. K, L and M edge energies (eV) for $10 \leq Z \leq 82$.

Element	Z	K	L1	L2	L3	M1	M2	M3	M4	M5
Ne	10	870.73	53.036	21.634	21.554					
Na	11	1080.15	75.161	38.382	38.212	7.118				
Mg	12	1312.30	100.75	58.159	57.904	8.766				
Al	13	1569.56	130.62	82.438	82.030	12.932	8.284			
Si	14	1850.26	163.72	110.59	109.10	15.293	8.474			
P	15	2154.24	199.79	141.10	139.51	18.096	10.444	13.417		
S	16	2481.72	239.15	174.70	172.91	21.625	11.986	14.187		
Cl	17	2832.76	281.80	211.49	209.09	25.784	13.725	15.184		
Ar	18	3207.44	327.31	251.55	249.54	30.020	16.135	15.967		
K	19	3616.22	386.25	304.25	301.62	41.244	24.440	24.728		
Ca	20	4049.35	450.46	361.79	358.37	55.574	35.032	34.668		
Sc	21	4501.68	510.11	416.25	411.53	62.831	40.525	38.755	10.893	
Ti	22	4977.93	573.33	473.85	467.55	70.806	47.058	43.465	11.970	
V	23	5478.29	639.78	534.69	526.50	79.019	53.868	48.286	12.951	
Cr	24	5995.66	702.31	591.60	581.78	81.440	54.925	48.557	8.842	
Mn	25	6552.12	782.94	665.92	654.02	96.447	66.732	59.458	14.603	13.581
Fe	26	7125.87	859.80	736.35	722.74	105.70	72.637	65.948	15.280	14.361
Co	27	7724.26	940.18	810.18	794.62	115.30	78.733	72.741	15.913	15.108
Ni	28	8347.42	1024.13	887.46	869.70	125.24	85.036	79.838	16.509	15.829
Cu	29	8987.96	1103.12	959.58	939.85	128.15	83.997	81.088	10.470	10.132
Zn	30	9668.55	1203.32	1052.33	1029.45	145.86	97.759	94.939	17.573	17.236
Ga	31	10377.76	1309.87	1152.66	1125.86	167.33	115.93	111.95	27.836	27.271
Ge	32	11113.83	1421.74	1258.15	1227.15	189.85	134.44	129.78	39.240	38.498
As	33	11876.74	1540.04	1368.90	1333.26	213.71	155.12	149.61	51.693	50.844
Se	34	12666.73	1663.23	1484.90	1444.18	238.86	176.46	170.23	65.251	64.298
Br	35	13483.86	1791.81	1606.17	1559.84	265.29	199.01	191.79	79.887	78.814
Kr	36	14328.07	1925.49	1732.49	1680.06	293.13	222.40	214.81	95.435	94.184
Rb	37	15207.74	2072.56	1871.98	1812.69	329.11	255.00	246.11	119.53	118.08
Sr	38	16115.27	2225.51	2017.46	1950.46	367.16	289.11	278.96	145.06	143.36
Y	39	17047.90	2380.76	2164.89	2089.76	403.24	321.13	309.46	168.69	166.50
Zr	40	18008.16	2541.11	2317.54	2233.28	440.13	354.04	340.71	192.94	190.17
Nb	41	18990.68	2700.53	2469.32	2375.02	471.81	381.84	366.62	212.22	208.45
Mo	42	20008.82	2873.84	2634.63	2529.71	512.96	418.94	401.75	240.11	235.99
Tc	43	21050.48	3046.63	2799.20	2682.91	549.27	451.03	431.74	262.68	258.46
Ru	44	22127.71	3232.70	2977.03	2848.19	594.42	491.97	470.24	293.96	289.13
Rh	45	23230.24	3420.89	3156.74	3014.48	644.27	530.42	506.10	322.42	317.19
Pd	46	24357.64	3609.88	3337.01	3180.38	675.91	565.61	538.08	346.64	341.41
Ag	47	25523.72	3814.28	3533.04	3360.71	726.28	610.91	580.64	381.99	376.11
Cd	48	26720.59	4026.07	3736.10	3546.84	778.98	659.17	625.46	419.39	412.78
In	49	27949.70	4246.17	3947.38	3739.91	835.27	711.06	673.55	460.04	452.63
Sn	50	29209.80	4473.20	4165.49	3938.45	893.72	765.07	723.43	502.44	494.16
Sb	51	30501.28	4707.33	4390.55	4142.58	954.45	821.25	775.23	546.68	537.47
Te	52	31824.30	4948.54	4622.56	4352.20	1017.37	879.57	828.83	592.68	582.47
I	53	33179.48	5197.16	4861.84	4567.52	1082.72	940.26	884.36	640.66	629.36
Xe	54	34566.52	5453.67	5108.11	4788.23	1150.46	1003.48	941.88	690.49	677.88
Cs	55	35991.94	5721.38	5367.06	5019.87	1225.24	1073.38	1006.17	747.01	733.28
Ba	56	37450.25	5997.72	5633.67	5257.36	1302.96	1146.30	1072.72	805.85	790.75
La	57	38939.47	6279.03	5905.22	5497.83	1380.41	1218.97	1138.56	864.01	847.38
Ce	58	40446.59	6550.37	6167.01	5726.48	1439.65	1273.91	1185.66	904.47	885.38
Pr	59	41994.13	6836.77	6443.60	5967.85	1509.86	1339.61	1243.22	954.91	933.57
Nd	60	43575.29	7130.17	6727.10	6213.91	1581.49	1406.76	1301.67	1006.26	982.49
Pm	61	45189.79	7430.18	7017.09	6464.16	1654.12	1474.94	1360.55	1058.03	1031.66
Sm	62	46839.05	7737.87	7314.76	6719.68	1728.73	1545.09	1420.92	1113.42	1082.12
Eu	63	48523.80	8053.71	7620.28	6980.47	1805.35	1617.23	1482.97	1165.45	1134.39
Gd	64	50251.69	8385.89	7942.02	7254.88	1893.73	1701.14	1555.98	1230.87	1197.10
Tb	65	51999.51	8708.14	8253.93	7516.62	1963.96	1766.48	1610.39	1276.81	1241.66
Dy	66	53792.37	9048.04	8583.26	7792.91	2046.91	1844.61	1676.63	1334.94	1297.59
Ho	67	55620.79	9395.16	8919.77	8073.32	2131.07	1923.89	1743.27	1393.36	1353.70
Er	68	57487.44	9750.65	9264.41	8358.67	2217.26	2005.10	1811.10	1452.89	1410.79
Tm	69	59391.18	10114.45	9617.34	8648.98	2305.52	2088.30	1880.12	1513.54	1468.87
Yb	70	61333.37	10486.85	9978.70	8944.26	2395.89	2173.27	1950.06	1575.13	1527.92
Lu	71	63322.75	10877.20	10357.44	9253.24	2498.79	2270.89	2031.57	1648.28	1597.47
Hf	72	65352.01	11277.17	10745.60	9567.88	2604.79	2371.19	2114.80	1723.22	1668.75
Ta	73	67431.96	11696.88	11153.23	9898.05	2723.65	2484.26	2209.83	1809.85	1751.56
W	74	69533.06	12106.90	11551.16	10214.26	2826.15	2580.91	2287.42	1879.07	1816.64
Re	75	71687.53	12537.49	11969.18	10546.35	2941.91	2690.67	2377.06	1960.15	1893.56
Os	76	73884.05	12978.42	12397.43	10884.15	3060.85	2803.54	2468.72	2043.16	1972.20
Ir	77	76117.51	13423.28	12829.39	11221.01	3176.34	2912.91	2555.72	2121.36	2045.83
Pt	78	78404.25	13888.71	13281.67	11573.12	3304.82	3035.10	2654.29	2211.14	2130.85
Au	79	80734.75	14362.22	13741.67	11927.79	3433.47	3157.40	2751.69	2299.65	2214.44
Hg	80	83111.29	14850.80	14216.92	12292.28	3569.65	3287.14	2855.18	2394.19	2303.69
Tl	81	85538.23	15353.13	14705.48	12664.39	3711.24	3422.15	2962.56	2492.56	2396.51
Pb	82	88012.80	15867.71	15206.13	13042.61	3856.58	3561.00	3072.45	2593.08	2491.37

Table 4. K, L and M edge energies (eV) for $83 \leq Z \leq 100$.

Element	A	Z	K	L1	L2	L3	M1	M2	M3	M4	M5
Bi	209	83	90536.51	16395.44	15719.66	13427.60	4006.91	3704.58	3185.04	2696.79	2588.88
Po	209	84	93109.98	16936.03	16245.84	13818.74	4161.18	3852.03	3300.18	2802.68	2688.43
At	210	85	95733.51	17489.71	16784.96	14216.04	4319.61	4003.59	3417.68	2910.88	2790.03
Rn	222	86	98408.15	18056.77	17337.39	14619.54	4482.30	4159.29	3537.91	3021.40	2893.65
Fr	223	87	101141.27	18642.43	17907.94	15033.78	4653.95	4323.91	3664.51	3138.80	3003.85
Ra	226	88	103927.76	19242.31	18492.62	15454.33	4830.18	4492.96	3793.88	3258.63	3116.18
Ac	227	89	106768.26	19855.19	19090.05	15879.45	5009.35	4664.88	3924.05	3379.20	3228.91
Th	232	90	109658.27	20481.60	19701.60	16310.28	5192.61	4841.01	4056.27	3501.77	3343.30
Pa	231	91	112601.71	21113.70	20318.13	16736.91	5369.32	5010.50	4179.35	3615.45	3448.18
U	233	92	115609.89	21766.16	20954.73	17174.24	5555.80	5189.62	4309.35	3736.01	3559.69
U	238	92	115608.15	21766.08	20954.96	17174.51	5555.97	5189.87	4309.61	3736.27	3559.95
Np	237	93	118674.25	22433.59	21606.63	17616.94	5746.09	5374.06	4442.80	3859.71	3673.96
Pu	239	94	121795.47	23111.95	22269.43	18060.03	5935.40	5554.62	4569.25	3976.60	3780.92
Pu	244	94	121786.72	23104.31	22262.01	18052.63	5927.93	5547.20	4561.84	3969.20	3773.51
Am	241	95	124984.82	23812.55	22954.04	18514.39	6135.39	5746.87	4705.18	4102.44	3896.88
Am	243	95	124984.20	23812.44	22954.03	18514.38	6135.36	5746.87	4705.17	4102.44	3896.88
Cm	245	96	128242.88	24535.46	23660.99	18979.69	6345.85	5949.72	4848.50	4235.78	4019.77
Cm	248	96	128241.03	24534.55	23660.27	18978.99	6345.08	5949.00	4847.79	4235.07	4019.06
Bk	249	97	131561.48	25270.96	24380.69	19445.77	6555.87	6152.06	4988.35	4365.45	4138.83
Bk	250	97	131560.96	25270.87	24380.68	19445.77	6555.85	6152.06	4988.35	4365.45	4138.83
Cf	249	98	134957.13	26033.44	25127.03	19925.99	6771.59	6360.00	5130.55	4497.36	4259.78
Cf	250	98	134956.96	26033.28	25126.86	19925.80	6771.56	6360.00	5130.55	4497.36	4259.78
Cf	251	98	134955.68	26032.87	25126.64	19925.63	6771.54	6360.00	5130.55	4497.36	4259.78
Es	251	99	138400.00	26792.14	25869.91	20389.43	6977.72	6558.34	5259.84	4616.21	4367.42
Fm	254	100	141927.40	27584.39	26646.49	20872.82	7204.03	6776.91	5405.71	4751.66	4491.06

Table 5. $1s$ Lamb shift from hydrogenlike ions and Kα transitions. All energies are in eV, except for hydrogen for which they are in MHz. Theoretical values are evaluated using reference [41].

Z	H-like			Ref.	Kα_1			Kα_2			Average			Theory
1	8172.80	±	0.05	[42]										8172.809
18	1.15	±	0.02	[32]	0.98	±	0.25	0.87	±	0.26	0.92	±	0.28	1.140
28	5.07	±	0.10	[33]	5.66	±	0.34	6.15	±	0.37	5.91	±	0.61	5.089
29					5.53	±	0.34	5.31	±	0.38	5.51	±	0.44	5.729
36	11.95	±	0.50	[37]	11.95	±	0.39	11.81	±	0.43	11.88	±	0.46	11.83
42					20.28	±	0.41	20.12	±	0.52	20.28	±	0.49	19.87
54	54	±	10	[38]	47.68	±	0.55	47.03	±	0.61	47.16	±	0.89	46.96
60					67.81	±	0.65	67.76	±	0.71	67.79	±	0.71	68.24
62					76.45	±	0.69	76.44	±	0.76	76.45	±	0.75	77.24
64					86.90	±	0.86	86.62	±	0.91	86.76	±	0.90	86.99
68					107.77	±	0.86	107.88	±	0.93	107.80	±	0.92	109.7
69					115.17	±	0.89	114.72	±	0.94	114.95	±	1.04	115.9
74					155.04	±	1.07	155.36	±	1.38	155.05	±	1.16	154.4
79	202.3	±	7.9	[34]	201.46	±	1.50	201.57	±	1.53	201.50	±	1.54	205.2
82					244.73	±	2.05	243.57	±	2.12	244.34	±	2.43	244.2
83					259.72	±	1.58	259.07	±	1.58	259.39	±	1.74	259.1
90					407.56	±	2.57	408.54	±	2.57	408.16	±	2.84	403.6
92	470	±	16	[5]	462.34	±	2.75	462.06	±	2.78	462.29	±	2.87	463.9
94					529.64	±	2.66	529.27	±	2.63	529.54	±	2.71	529.7
96					622.01	±	3.76	621.33	±	3.64	621.67	±	3.62	610.2
98					710.06	±	5.85	708.94	±	5.73	709.50	±	4.98	702.9

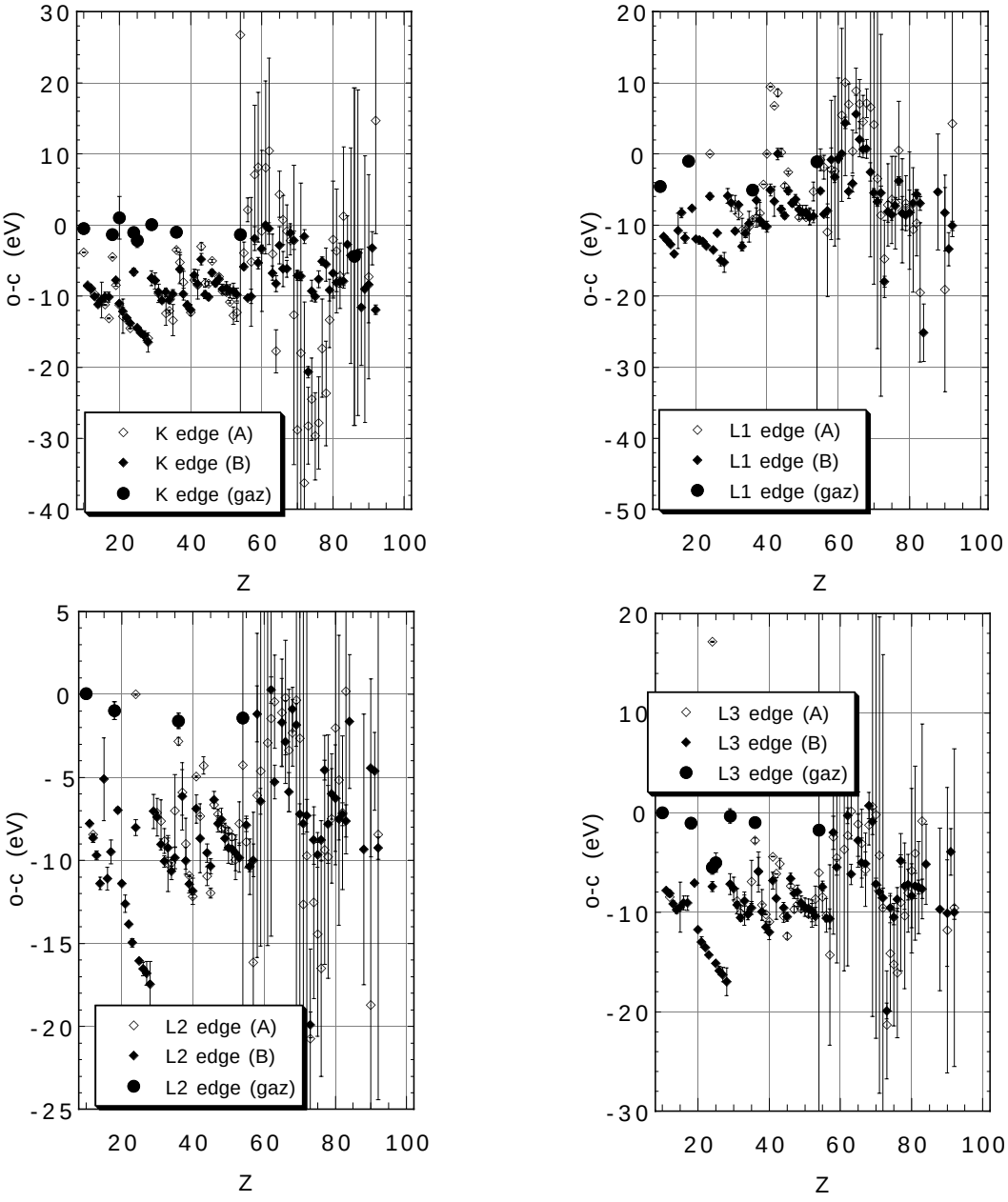

Fig. 7. Difference between experimental and theoretical ionization energies for the K, L_1, L_2, L_3 shells (o-c, observed-calculated). Metal vapor data are from reference [31].

between theory and experiment is very good in general for Kα transitions (Fig. 8), and no systematic deviation can be observed. As the nuclear size correction and QED corrections affect more strongly the $1s$ state, this agreement is a good indication that these effects are taken into account properly. In contrast the comparison between theory and experiment for Kβ transitions is rather poor in the region $55 \leq Z \leq 84$. For L lines it is even more difficult to get general trends. There is a clear linearly increasing deviation between experiment and theory for Lα_1 lines in the region $80 \leq Z \leq 91$ which suspiciously looks like an artifact in the X-ray tables. For all the other L lines, data are too scarce or too scattered at high-Z to enable to draw clear conclusions. In general the few recent measurements made by T. Mooney at N.I.S.T. [30] (displayed as reference data) are in good agreement with theory (within 1 eV).

For unstable elements (Tc and elements with atomic number $84 \leq Z \leq 89$ and the highest-Z transuranic elements), uncorrected theory is certainly much more reliable than the data from Bearden's table, most of which have been obtained by interpolation from adjacent elements. For $84 \leq Z \leq 89$ the lack of data on nuclear size constitute the most sizeable source of uncertainty. As discussed in our earlier work, measurements with muonic atoms have proven that for $Z \geq 90$, the nuclear deformation gives an increase of the mean spherical charge radius of the nucleus

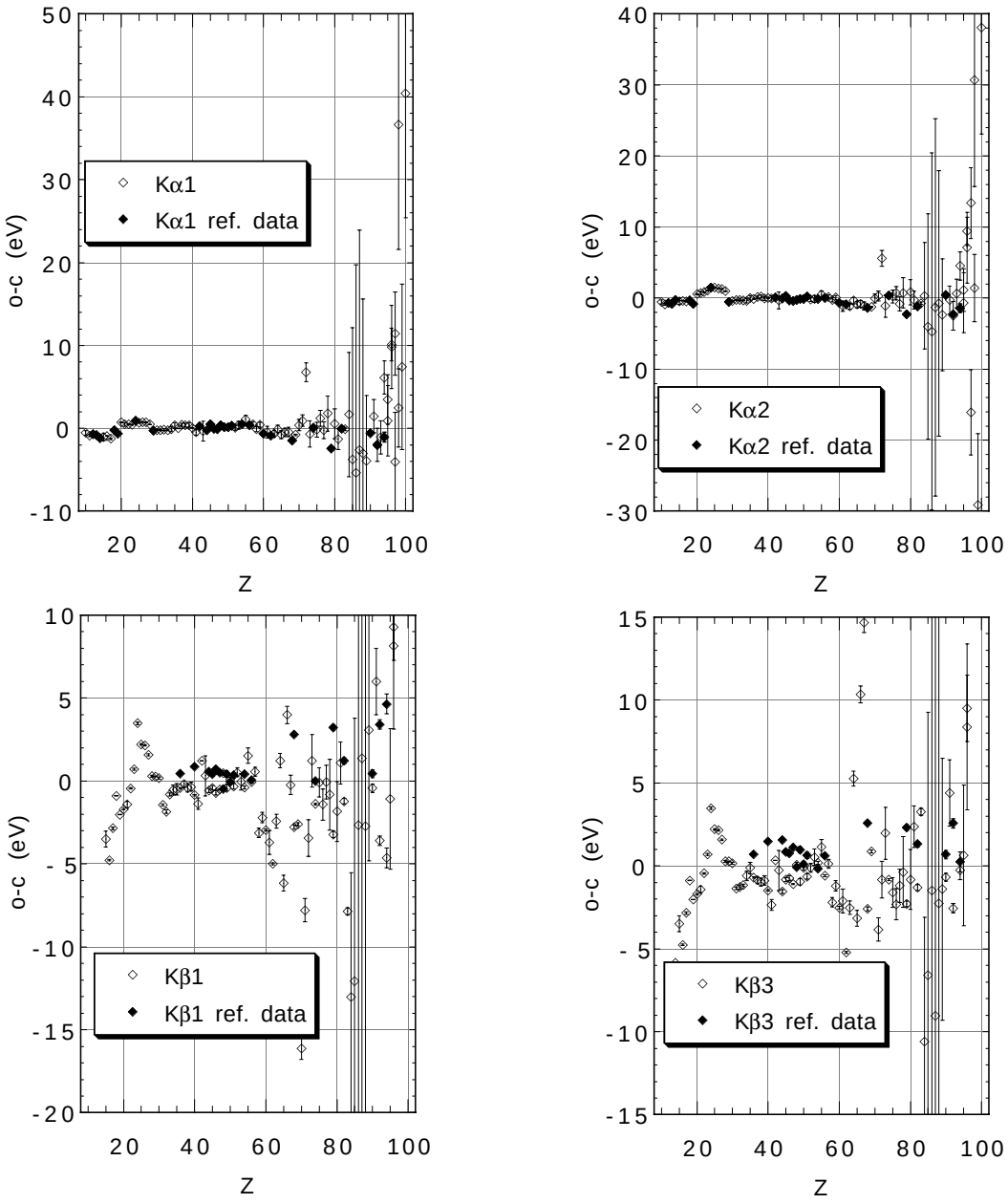

Fig. 8. Difference between experimental and theoretical energies (o-c) for Kα1, Kα2, Kβ1, Kβ3 transitions.

by 0.11 Fm. Such an increase does not appear for Bi, but what happens between Bi and Th is not known.

3 Determination of the one-electron 1s Lamb Shift in heavy elements

In the last 15 years, there has been a great push to measure $1s$ and $2s$ Lamb shifts in heavy hydrogenlike [5,32–38] or lithiumlike ions from Ar to U. The hydrogenlike ions are simple systems from which one expects the best fundamental test of Quantum-Electrodynamics in strong Coulomb field. In systems with more electrons the result can be obscured by many electron effects. However because of the difficulty to produce large enough quantities of hydrogenlike ions in storage rings or Electron-Beam Ion traps (EBIT) for high resolution spectroscopy, there are no result available with precision better than a few percent of the $1s$ Lamb shift. Besides, it is unlikely that elements heavier than uranium can be studied. In contrast there is the large corpus of high precision measurement (few ppm accuracy) of Kα transition energy, that can now be used, combined with the present calculation, to extract $1s$ Lamb shift up to $Z = 96$. Here the main uncertainty lies in the uncalculated many-body and many-electron QED effects. However the order of magnitude of these uncalculated terms is known, and can be used to provide an error estimate. From calculation made on Xe

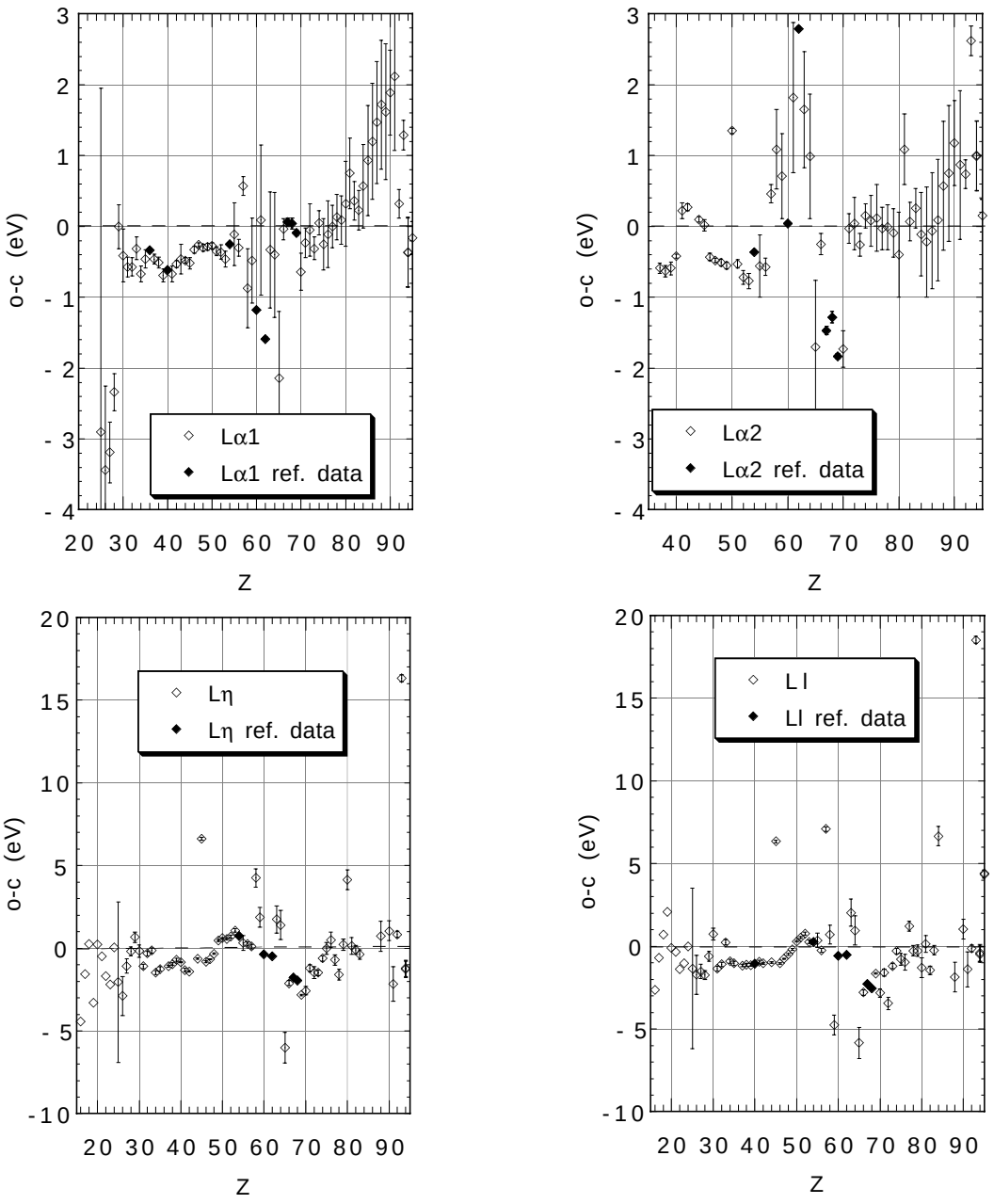

Fig. 9. Difference between experimental and theoretical energies (o-c) for Lα1, Lα2, Lη, Ll transitions. Reference data are from reference [30].

[2], we estimate the uncertainty due to uncalculated many-body effects to 10% of the sum of the absolute value of the Coulomb and Magnetic correlation, and of the Auger and core-core corrections. Then we quadratically combine this with the experimental uncertainty, the missing box-diagram contribution (estimated from [39,40]). Finally we estimate the uncertainty in two-electron radiative corrections to 15% of the Welton estimate, as this contribution was always found to be more precise than 10% in simple systems. To extract this experimental 1s Lamb shift one needs only to calculate the Kα transition energy without any one-electron QED correction for 1s electrons. One-electron QED corrections for all other shell will cancel in the transition energy. The results are presented in Table 5 and plotted on Figure 11, together with the most accurate Lamb shift determination in hydrogenlike ions. One can see that for $96 \geq Z \geq 54$ the relative precision of this Lamb shift determination is below 1%, a situation much better than the situation for hydrogenlike ions.

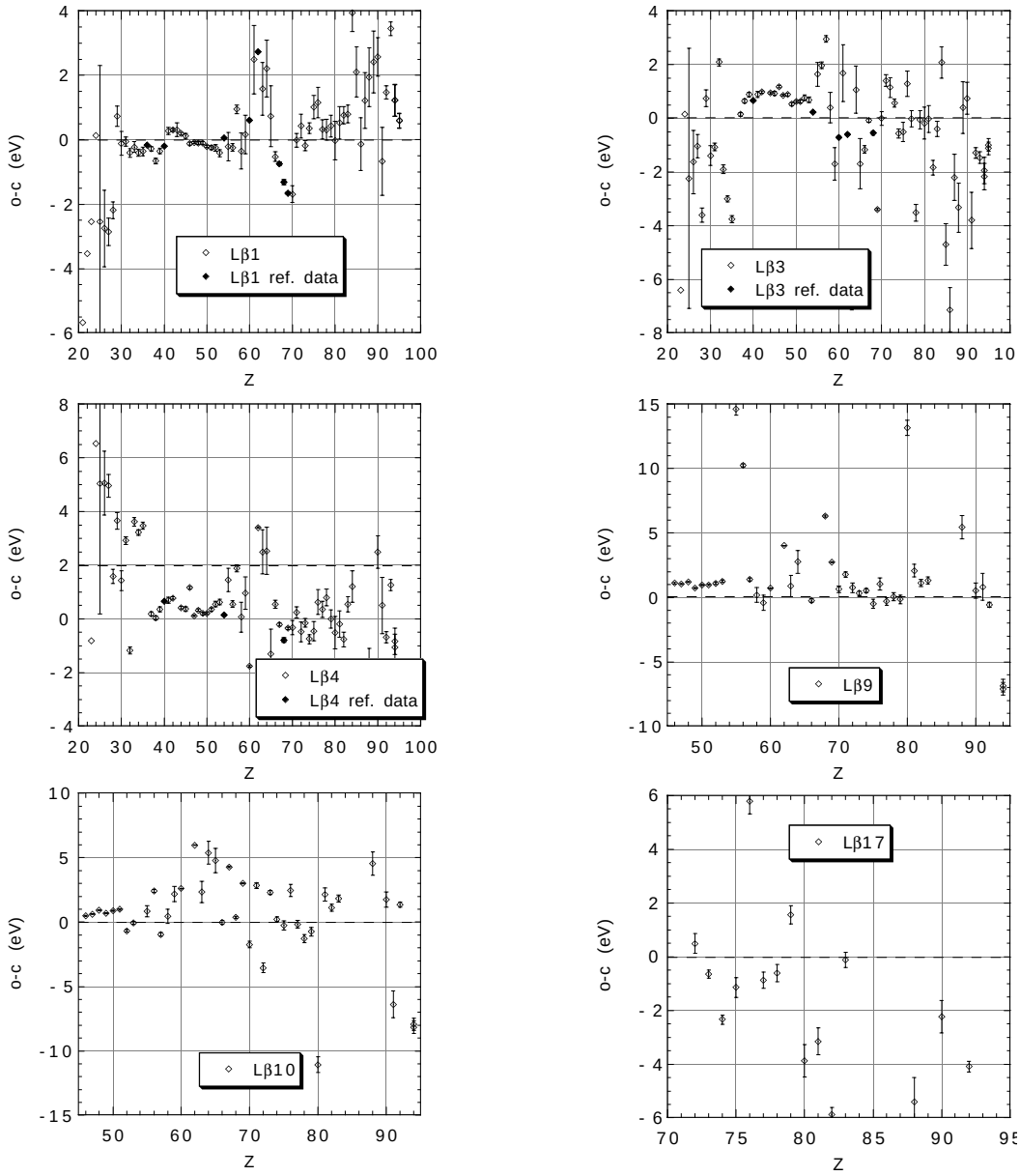

Fig. 10. Difference between experimental and theoretical energies (o-c) for Lβ1, Lβ3, Lβ4, Lβ9, Lβ10, Lβ17 transitions. Reference data are from reference [30].

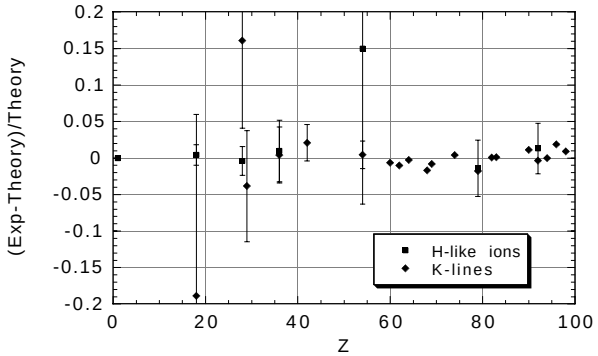

Fig. 11. Comparison between theoretical and experimental determination of the 1s Lamb shift.

4 Conclusion

In this paper we have evaluated K, L and M ionization energies for atoms with $10 \leq Z \leq 100$. Relativistic, Many-body and QED corrections have been evaluated with very high accuracy. The K and L ionization energies have been compared with experiment on atoms and solids. Our atomic calculations reproduce experiments on atoms within a few eV, and show the size of solid state contributions to the other measurements. With the calculations we are able to predict many K and L transitions energy. The agreement in places where precise measurements exist is very good, often below 1 eV. In many instances the theoretical values are more accurate than experimental ones, as many lines have been measured when crystal spectroscopy technology was still very primitive. The same thing happens for elements for which no long-lived isotope exist. As it is unrealistic to expect that a complete remeasurements program will be undertaken anytime soon these calculations constitute a firm and simple foundation for a critical reevaluation of X-rays tables. Such a task has been started and preliminary results are very encouraging [26].

We wish to thank Dr. R.D. Deslattes and Dr. E.G. Kessler, Jr., for many discussions which were essential to make this work possible. One of us (P.I.) is very grateful to Dr. R.D. Deslattes for providing support for several stays at N.I.S.T. Funding for travel was provided by N.A.T.O. grant CRG-960623. E.L. is grateful to the Swedish Natural Science Research Council (NFR) for support.

References

1. P. Indelicato, E. Lindroth, Phys. Rev. A **46**, 2426 (1992).
2. T. Mooney, E. Lindroth, P. Indelicato, E. Kessler, R. Deslattes, Phys. Rev. A **45**, 1531 (1992).
3. E. Lindroth, P. Indelicato, Phys. Scr. T **46**, 139 (1993).
4. E. Lindroth, P. Indelicato, Nucl. Instrum. Methods B **87**, 22 (1994).
5. H.F. Beyer, G. Menzel, D. Liesen, A. Gallus, F. Bosch, R.D. Deslattes, P. Indelicato, T. Stöhlker, O. Klepper, R. Moshammer, F. Nolden, H. Eickhoff, B. Franzke, M. Steck, Z. Phys. D **35**, 169 (1995).
6. H.F. Beyer, IEEE Trans. Instrum. Meas. **44**, 510 (1995).
7. E.G. Kessler, R.D. Deslattes, D. Girard, W. Schwitz, L. Jacobs, O. Renner, Phys. Rev. A **26**, 2696 (1982).
8. P. Indelicato E. Lindroth, Comments At. Mol. Phys. **32**, 197 (1996).
9. J.A. Bearden, Rev. Mod. Phys. **39**, 78 (1967).
10. E. Lindroth, Phys. Rev. A **49**, 4473 (1994).
11. W. Zong, R. Schuch, E. Lindroth, H. Gao, D.R. DeWitt, S. Asp, H. Danared, Phys. Rev. A **56**, 386 (1997).
12. J.D. Zumbro, R.A. Naumann, M.V. Hoehn, W. Reuter, E.B. Shera, C.E.B. Jr., Y. Tanaka, Phys. Lett. B **167**, 383 (1986).
13. M.W. Johnson, E.B. Shera, M.V. Hoehn, R.A. Naumann, J.D. Zumbro, C.E. Bemis, Phys. Lett. B **161**, 75 (1985).
14. J.D. Zumbro, E.B. Shera, Y. Tanaka, J.C. Bemis, R.A. Naumann, M.V. Hoehn, W. Reuter, R.M. Steffen, Phys. Rev. Lett. **53**, 1888 (1984).
15. S.A. Blundell, W.R. Johnson, J. Sapirstein, Phys. Rev. A **41**, 1698 (1990).
16. P. Indelicato, in *X-Ray and Inner-Shell Processes* (AIP, New-York, 1990), Vol. 215, pp. 591–601.
17. G. Plunien, B. Müller, W. Greiner, G. Soff, Phys. Rev. A **39**, 5428 (1989).
18. G. Plunien, B. Muller, W. Greiner, G. Soff, Phys. Rev. A **43**, 5853 (1991).
19. G. Plunien G. Soff, Phys. Rev. A **53**, 4614 (1996).
20. P.J. Mohr, Ann. Phys. (N.Y.) **88**, 52 (1974).
21. P.J. Mohr Y.-K. Kim, Phy. Rev. A **45**, 2727 (1992).
22. P.J. Mohr G. Soff, Phys. Rev. Lett. **70**, 158 (1993).
23. H. Person, I. Lindgren, L. Labzowsky, G. Plunien, T. Beier, G. Soff, Phys. Rev. A **54**, 2805 (1996).
24. I. Lindgren, H. Persson, S. Salomonson, V. Karasiev, L. Labzowsky, A. Mitrushenkov, M. Tokman, J. Phys. B: At. Mol. Phys. **26**, L503 (1993).
25. S.A. Blundell, P.J. Mohr, W.R. Johnson, J. Sapirstein, Phys. Rev. A **48**, 2615 (1993).
26. R.D. Deslattes, J.E. Kessler, P. Indelicato, E. Lindroth, in *International Tables for Crystallography*, edited by T. Price (Kluwer Academic Publishers, London, 1997), Vol. C, pp. 11–22.
27. J. Schweppes, R.D. Deslattes, T. Mooney, C.J. Powell, J. Electron Spectrosc. Relat. Phenom. **67**, 463 (1994).
28. J. Härtwig, G. Hölzer, J. Wolf, E. Förster, J. Appl. Cryst. **26**, 539 (1993).
29. R. Deslattes (private communication, 1990).
30. T. Mooney (private communication, 1990).
31. U. Arpt, B.M. Lagutin, G. Materlik, I.D. Petrov, B. Sonntag, V.L. Sukhorukov, J. Phys. B: At. Mol. Opt. Phys. **26**, 4381 (1993).
32. H.F. Beyer, R.D. Deslattes, F. Folkmann, R.E. LaVilla, J. Phys. B: At. Mol. Opt. Phys. **18**, 207 (1985).
33. H. Beyer, P. Indelicato, H. Finlayson, D. Liesen, R.D. Deslattes, Phys. Rev. A **43**, 223 (1991).
34. H.F. Beyer, D. Liesen, F. Bosch, K.D. Finlayson, M. Jung, O. Klepper, R. Moshammer, K. Beckert, H. Eickhoff, B. Franzke, F. Nolden, P. Spädtke, M. Steck, G. Menzel, R.D. Deslattes, Phys. Lett. A **184**, 435 (1994).
35. H.F. Beyer, K.D. Finlayson, D. Liesen, P. Indelicato, C.T. Chantler, R.D. Deslattes, J. Schweppe, F. Bosch, M. Jung, O. Klepper, W. König, R. Moshammer, K. Beckert, H. Heuckhoff, B. Franzke, A. Gruber, F. Nolden, P. Spädtke, M. Steck, J. Phys. B: At. Mol. Opt. Phys. **26**, 1557 (1993).
36. J.P. Briand, M. Tavernier, P. Indelicato, R. Marrus, H. Gould, Phys. Rev. Lett. **50**, 832 (1983).
37. M. Tavernier, J.P. Briand, P. Indelicato, D. Liesen, P. Richard, J. Phys. B: At. Mol. Opt. Phys. **18**, L327 (1985).
38. J.P. Briand, P. Indelicato, A. Simionovici, V.S. Vicente, D. Liesen, D. Dietrich, Europhys. Lett. **9**, 225 (1989).
39. I. Lindgren, H. Persson, S. Salomonson, Phys. Rev. A **51**, 1167 (1995).
40. S.A. Blundell, P.J. Mohr, W.R. Johnson, J. Sapirstein, Phys. Rev. A **48**, 2615 (1993).
41. P.J. Mohr, in *Handbook of Atomic Physics* (American Institute of Physics, New-York, 1996), p. 125.
42. S. Bourzeix, B. de Bauvoir, F. Nez, M.D. Plimmer, F. de Tomazi, L. Julien, F. Biraben, D.N. Stacey, Phys. Rev. Lett. **76**, 384 (1996).